Laser additive manufacturing of embedded electronics

12

R.C.Y. Auyeung, H. Kim, S. Mathews, N. Charipar, A. Piqué
Naval Research Laboratory, Washington, DC, United States

12.1 Introduction

Doing more with less has been the driving force behind many of the advances in microelectronics for many decades. The aerospace, medical, consumer, and military markets seek electronics components with increased performance, portability, and versatility while reducing their physical footprint, power consumption, and thermal budget. This theme is nowhere more evident than in the rapidly maturing field of flexible or conformal electronics, which requires thinner and smaller components to take full advantage of a flexible substrate [1]. All of these drivers, of course, must result in a product with a cost-to-benefit ratio that is advantageous in their respective markets.

Miniaturization at the integrated circuit (IC) level has been advancing dramatically since the invention of the transistor, with a 1000-times decrease in the node dimension since 1970. By comparison, the printed circuit assembly (or board) (PCA) that integrates these chips with other heterogeneous components has decreased by only five times using the interconnect pitch as the metric [2]. A significant portion of today's PCAs contains about 80% passive components, of which most are resistors and capacitors, that occupy over 40% of the PCA surface area [3,4]. These discrete components (such as memory, passive elements, and other processing elements) could be combined into a single chip [application-specific integrated circuit (ASIC)] or assembled into a three-dimensional (3D) architecture (eg, die stacking). However, these are costly and time-consuming techniques that do not easily accommodate design changes once finalized.

Further miniaturization of the PCA can occur by utilizing surface-mount devices (SMDs) for many of the passive elements and narrowing the interconnect pitch; however, the ultimate gains in component density can be achieved by burying or embedding these components into the substrate to create a vertically integrated packaging and design architecture. Benefits of embedding electronics include shorter resistor-capacitor (RC) time delays, reduced inductance, better shielding, new functionalities/architectures on novel (eg, flexible) substrates, proprietary design protection and weight savings. The challenges of effectively embedding electronics at the highest possible density require careful handling of small and ultrathin bare dies and connecting them to the circuitry with high-quality fine-pitch interconnects.

Currently, these miniature components, such as SMDs, semiconductor bare (ie, unpackaged) dies, and microelectromechanical systems (MEMSs), are carefully handled and precisely placed on a substrate with "pick-and-place" or SMD placement machines. However as their areal size shrinks below a few hundred microns and

Laser Additive Manufacturing. http://dx.doi.org/10.1016/B978-0-08-100433-3.00012-9
Copyright © 2017 Elsevier Ltd. All rights reserved.

thickness drops below 50 μm, these dies can be easily damaged or mishandled by these machines. Various die pickup and transfer methods have been adapted for ultrathin dies, but further development is needed to increase the yield, speed, and range of die thickness and size that can be used in the process [5]. Laser-based methods that do not directly contact the receiving surface can transfer millimeter- to micron-sized components from a donor substrate (carrier) to a receiver substrate without damage; these techniques are reviewed in the next section.

Once these discrete components are placed inside the substrate, they are interconnected and encapsulated using methods such as PCA lamination (which includes flip-chip and micro-via processes for chip−substrate connections), or low-temperature cofired ceramic. [Traditional wire-bonding is not suitable because their bond pads (tens of micrometers wide) and loop heights (>75 μm) limit the packing density of embedded components [6]]. These techniques build the design layer by layer (and could be considered as a basic form of additive manufacturing), but unfortunately they have long design/build cycles or may expose components to high temperatures (<1000°C). In addition, both these methods use batch patterning processes such as screen printing and photolithography, which do not allow quick design changes, have limited feature size resolution (screen print), consume excessive material, or involve costly and complex steps (eg, photomask).

Alternatively, instead of placing preexisting devices inside a substrate, functional components can be directly fabricated and connected inside a substrate by additive manufacturing. Because this technique does not depend on fixed masks or templates, design changes are quick, and rapid prototyping can be performed [7,8]. In particular, using a laser additive manufacturing technique called laser direct write (LDW) enables the capabilities of additive manufacturing (laser transfer of dies and thin-film structures) and subtractive manufacturing (laser micromachining) to be combined into a single tool [9,10]. This is a unique capability that no other additive manufacturing tool possesses. (As used in this chapter and in the literature, "LDW" refers to all laser processes that can add, modify, or remove material in specific locations in/on a substrate and is usually performed under ambient conditions). LDW developed from the laser-induced forward transfer (LIFT) process [11], which was originally used to print copper lines in a vacuum. (LIFT, as used in this chapter, is used to describe laser processes that strictly add material or structures to a substrate). LIFT has been demonstrated for many functional materials such as metals, oxides, and organics over a wide range of viscosities without affecting their functionality. By laser-transferring functional materials in exact locations and geometries, LIFT can effectively shrink and replace SMDs with "print-on-demand" components with (ideally) similar performance. As an example of LDW's capability, the pocket in the substrate that houses the die could be created by laser micromachining, then the die can be placed into the pocket by laser device transfer and the interconnects from the circuit to the die printed by laser forward transfer.

This chapter focuses on the different additive processes that LDW can be used to embed electronics. (Subtractive LDW techniques such as laser micromachining have been firmly adopted by industry and will not be discussed in detail). First, the different techniques used to laser transfer prefabricated discrete components

(eg, SMD, die) from a donor to a receiving substrate are presented. Second, LIFT of functional materials that could replace discrete elements, such as metallic interconnects, microbatteries, and photovoltaics, are discussed. Third, circuit elements from the first two discussions (discretes and interconnects) are combined in examples of completed circuits using laser transfer. The combined capability of laser additive manufacturing to transfer discrete components and/or print their counterparts in precise locations (as well as to remove material) will enable the rapid prototyping of embedded electronics in both form and function, thus reducing time to market in manufacturing as well as advancing new nontraditional applications.

12.2 Laser-induced forward transfer of discrete components

Laser-based transfer of discrete components from a donor to a receiving substrate typically involves three steps in the following order: release, propulsion across a gap, and emplacement. A laser pulse could provide energy for all three steps or just be used for release and then be assisted by other forces (eg, gravity, magnetic forces) for transfer to the substrate. Other laser-based transfer processes such as laser release [12] or laser debonding [13], in which structures are released from a donor substrate by laser ablation or heating after first making physical contact with a receiving substrate, are not discussed in this chapter.

A history of the LIFT of microstructures along with selected metrics is shown in Table 12.1. In the first demonstration [14], prefabricated nickel and MEMS-like microstructures were first attached to a polymer sacrificial layer coated on an ultraviolet (UV)−transparent donor substrate. Upon absorption of an incident 248-nm laser pulse, they were released and propelled across a small gap by gases resulting from ablation of the polymer layer. Transfers of 100-μm^2 "pads" onto complementary "frames" and a laser-assembled "wobble" motor were demonstrated. Although it was noted that the placement accuracy may require structural features to guide the trajectory of the transfer, a placement error of $\sim$40 μm could be estimated from the images of the transferred frames onto the pads.

In another study, an infrared (IR) laser pulse ($\lambda = 1064$ nm, 45 ns) with a flat-top spatial profile was used to release silicon bare dies (tiles) from a polyvinyl chloride (PVC) tape carrier [15]. The authors suggested that since the tape was IR-transparent, the laser energy was absorbed by the silicon, which, through heat conduction, melted and vaporized part of the tape adjacent to the silicon, thereby releasing the die. In this process, the nonactive (back) side of the silicon faced the laser pulse, so it would have been difficult to establish electrical connections in this configuration since precise die alignment would have been needed. No receiving substrates were used, so the placement accuracy could not be evaluated. A thermal model was developed that predicted a releasing fluence threshold of 2.9 J/cm^2, which agreed reasonably with the observed value of 3.7 J/cm^2. The model also predicted a die-release speed of $\sim$15 m/s at 4.5 J/cm^2, which roughly agreed with the observed value of $\sim$12 m/s, but the

Table 12.1 Historical summary of laser-assisted die transfer processes

Laser process	Laser λ (nm)	Fluence (J/cm^2)	Structures transferred	Accuracy (μm)	References
Ablative: DRL (single pulse)	KrF 248	0.1	Ni (100 × 100 × 15 μm) Wobble motor demo (1 mm ø)	~40[a]	[14]
Thermal: PVC carrier (single pulse)	YAG 1064	4.5 (45 ns)	Silicon bare die (200 × 200 × 150 μm)	–	[15]
Thermal: PET carrier + gas-filled adhesive (single pulse)	YAG 532	6 (0.2 ms)	Silicon (300 × 300 × 130 μm)	35[a]	[16]
Ablative: DRL (L&P) (single pulse)	KrF 248	0.1–1.4 (15 ns)	SMD (1 × 0.5 mm), bare die IC (LM555, 2.6 mm^2), LED (0.25 mm^2), Silicon (1 mm^2 × 10 μm)	<50	[17,18]
			Bare dies (LM555, LED array), microgear, silicon beam, silver ink	–	[19]
	YAG 355	0.2–0.3 (35 ns)	Copper metal interconnects (1 mm × 100 μm × 12.5 μm)	–	[20]
Ablative/mechanical: dual-DRL/blister (multi-pulse)	YAG 355	<10[a]	RFID tag (680 μm^2 × 65 μm), silicon (510 μm^2 × 65 μm)	~50	[21,22]
		4	Silicon (670 μm^2 × 50 μm)	~25	[23]
			Silicon (350 μm^2 × 20 μm), RFID-embedded paper	–	[24]
Thermal: CTE (single pulse)	Diode 805	3.5[a] (4 ms)	Silicon (100 μm^2 × 3 μm), LED	<5[a]	[25,26]
Ablative DRL/ magnetic(single or multi-pulse)	YAG 266	–	Silicon (1 mm^2 × 50 μm), silicon (2 mm^2 × 50 μm)	40–50 10–100	[27]

DRL, dynamic release layer; *LED*, light-emitting diode; *L&P*, lase and place; *RFID*, radiofrequency identification; *PVC*, polyvinyl chloride; *PET*, polyethylene terephthalate; *CTE*, coefficient of thermal expansion; *SMD*, surface mount devices.
[a]Estimated.

predicted speeds were underestimated at higher fluences. It was reported that the laser fluence of 4.5 J/cm^2 to release the die was below the calculated fluence threshold of 17 J/cm^2 for silicon damage, but no experimental evidence was given. A fluence of 4.5 J/cm^2 in 45 ns lies very close to the ablation fluence threshold of 6−8 J/cm^2 in silicon for a single 1062-nm, 65-ns laser pulse [28]. This process could have operated just below the ablation threshold and provided gradual heating of the PVC tape, resulting in a more predictable transfer.

In a subsequent study, the same group used high-speed video imaging to study the laser release of silicon bare die from a carrier tape under separate mechanisms: ablative and thermal [16]. Using 1064-nm pulses for the ablative and thermal regimes (nanoseconds and milliseconds, respectively), the released die velocity decreased by a factor of 10 in the thermal case, but the releasing velocity and angle were unstable because of nonlinear IR absorption in silicon. Therefore, a frequency-doubled neodymium-doped yttrium aluminium garnet (Nd:YAG) (532 nm, 0.2 ms) laser pulse was used to minimize this nonlinear absorption, and a flat-top beam spatial profile was used to reduce beam inhomogeneities. By examining the die release from different camera angles, a die placement accuracy of ±35 μm within a 9 degree release angle was calculated, assuming a donor-receiver gap of 0.2 mm. This measurement was made with no receiving substrate in close proximity. Die velocities were measured ranging from 0.7 to 1 m/s.

To that point in time, only discrete demonstrator components had been laser transferred to a receiving surface, but their functionality was not verified after the transfer. At the Naval Research Laboratory (NRL), by selecting the proper type and amount of sacrificial polymer to act as a dynamic release layer (DRL), the "lase-and-place" (L&P) process was used to transfer structures and devices (LM555 timer chip, light-emitting diode (LED), SMD resistors, capacitors) with sizes ranging from 0.1 to >6 mm^2, thicknesses from 500 to 10 μm, and placement accuracies of 50 μm [17] onto receiving substrates. These devices were then verified to be fully functional after the laser transfer. In addition, the LIFT process was used to directly print a wide array of electronic materials such as metals, dielectrics, nanocomposites, polymers, and electrochemically active compounds for applications such as interconnects, resistors, microbatteries, and photovoltaics. These components were also shown to have good functional properties after the laser printing process. Note that the laser fluences used in the NRL transfer process were near the lower range of fluences used in the other techniques. These lower fluences were achieved through careful DRL engineering (to create "pedestals" underneath the component) and/or using a shorter wavelength laser pulse to minimize the absorption depth; this may help explain the high placement accuracy and lack of damage to the die when using this technique. A recent application of the L&P process was in the transfer of freestanding copper interconnects between an array of capacitors [20]. Flat and bent copper metal strips (12.5 μm thick) were laser transferred to connect four capacitors in parallel with no degradation in performance. A more detailed discussion of the laser transfer work at NRL is presented in subsequent sections.

A different approach to using LIFT to transfer dies used a mechanical rather than an ablative or thermal process [21] to propel the die toward the receiving substrate. Here, a double DRL on the donor substrate consisted of a laser-absorbing polyimide layer

and an adhesive layer, which held the die. Upon 355-nm laser illumination, a small region of the DRL was vaporized, which created a blister without any rupture of the layers. This confined ablation of the DRL allowed the blister to act as a mechanical actuator that gently propelled the die toward the receiving substrate. Laser beam parameters (power, scan speed) had to be carefully chosen to avoid rupture of the DRL, which would contaminate or damage the surface of the die. The placement accuracy on a receiving substrate was studied as a function of laser parameters, adhesive layer properties, and dicing method (laser vs. reactive ion etching) [23]. A mean displacement accuracy of $\sim 22-27$ μm was found for a 670-μm^2 × 50-μm silicon die. Limited by their available laser options, multiple laser pulses were used to create the blister, which may not have resulted in a uniform release had a single laser pulse been used. It was also noted that the properties of the adhesive layer significantly affected the transfer yield and placement accuracy.

Another variant of the LIFT process, which did not use ablation of a sacrificial layer to drive die transfer, exploited the difference in coefficients of thermal expansion (CTEs) between the donor substrate and the die itself [25]. Here, a patterned elastomeric [polydimethylsiloxane (PDMS)] transfer tool (stamp), picked up a 100-μm^2 × 3-μm silicon die and positioned it over, but not touching, the receiving substrate (<10-μm gap). A 4-ms pulse from a continuous wave (cw) IR ($\lambda = 805$ nm) laser diode was then focused through the IR-transparent tool onto the die, which in turn heated the PDMS tool by conduction. Because of a two-order-of-magnitude difference between the CTEs of the PDMS and silicon, the interface is stressed and eventually results in delamination and release of the die from the tool. Transfers of silicon die pyramid structures and a functioning LED were demonstrated, as were depositions onto structured, curved (liquid droplet), and recessed surfaces [26]. A study of the placement accuracy showed that errors were insignificant below a separation of 20 μm between the die and the receiving surface. The IR laser fluence was estimated to be 3.5 J/cm^2 (assuming 2.5 W in a 600-μm-diameter spot) but delivered over 4 ms onto the die. An advantage of this technique was the ability of the stamp to pick up structures from another substrate and then (laser) release them onto another without any damage; this reusability of the transfer tool makes it similar to a pick-and-place process. Some disadvantages of this technique are that thicker dies (>10 μm) may not transfer reliably because of interfacial temperature requirements, the size of the pattern on the stamp must be >1.5 times the die size for reliable placement accuracy, and a "solid" die with a large interfacial surface area with the stamp transfers more reliably than one that is highly structured (eg, annulus) [29]. In a production environment, this may require stamp patterns to be specialized for each die.

The previous laser-transfer techniques focused on different release mechanisms for the die: ablative, thermal, mechanical, or some combination thereof. In another approach the trajectory of the die across the gap was controlled by a magnetic field *after* release from a DRL [27]. Here, different nickel patterns were deposited on square silicon chips to guide their trajectory in an external magnetic field. Single 266-nm pulses were used to transfer 1-mm^2 × 50-μm chips onto water-filled recesses on a glass coverslip. Multiple pulses scanning three concentric rings were required to release a 2-mm^2 × 50-μm chip. The placement accuracy on the receiving substrate

depended greatly on the initial release angle of the die (hence the wide range of accuracy values shown in Table 12.1), but the placement accuracy was found to be 40 μm (1 mm^2) and 10 μm (2 mm^2) for a specific initial release angle and nickel pattern, respectively, on the chip.

In summary, a variety of laser-assisted mechanisms have been used to transfer dies onto a receiving substrate. Laser ablation, heating, or mechanical processes were used to release the die and then propel it to the receiving substrate by residual kinetic energy or gravitational or magnetic forces. For ablation, a thin sacrificial DRL between the die and the donor substrate was used to absorb the laser energy, which was then converted into the kinetic energy of the die. The lasers used in Table 12.1 operated at UV, visible, or IR wavelengths and typically exposed the dies to fluences ranging from 0.1 to many Joules per centimeter square. For the excimer (KrF) and frequency-converted YAG lasers, their pulse widths at full-width-half-maximum (FWHM) are typically in the tens of nanoseconds, and this results in incident peak intensities of many megawatts per centimeter square. This high peak intensity is required to ablate and vaporize enough of the DRL to release and propel the die, but at the same time it could run the risk of damaging the die (especially the active side, which includes the contact pads). Some of the techniques in Table 12.1 attempted to mitigate this high intensity requirement by using (1) DRL engineering to lower the ablation threshold for transfer (NRL) and (2) confined ablation within the DRL to shield the die from exposure to the laser and to create a blister for mechanical actuation [21].

The other two mechanisms for releasing the die were thermally and mechanically based, which do not require high peak intensities and can be achieved with the use of longer pulsed and cw lasers. In Table 12.1, the thermal-PET method used peak intensities of 30 kW/cm^2 (6 J/cm^2 in 0.2 ms), whereas the thermal-CTE method used 880 W/cm^2 (3.5 J/cm^2 in 4 ms). Note that the definitions of *peak intensity* and *average intensity* are identical for cw lasers. These lower peak intensities lie below the ablation threshold of many materials and would minimize any damage to the die.

The placement accuracy of the transferred dies was typically 40−50 μm for the ablative techniques and a few tens of micrometers for the thermal/mechanical processes. Some angular misalignment was present in many of the techniques as well. The higher fluences required in ablative rather than thermal processes resulted in higher transfer speeds that increased the translational and rotational motion of the die as it reached the receiving substrate. Minimizing the donor−substrate gap may decrease these displacement and rotational errors.

The viability of each of the techniques in Table 12.1 could be demonstrated by measuring the functional properties of the components after laser transfer; however, this was done in only three of them: ablative (DRL-L&P), ablative (blister), and thermal (CTE). The first and the third techniques transferred the die or chip with the active side up (facing the laser pulse), whereas the second method used a “flip chip” configuration in which the back side faced the laser. It is important to note that all three methods used relatively low fluences (intensities) or shielded the die from most of the laser energy (blister). This lower fluence or peak intensity would have minimized any possible damage to the active side. In the blister technique, interconnects were made to an radiofrequency identification (RFID) tag by stencil-printing conductive

paste into vias or patterns on a substrate after laser transfer. In the thermal (CTE) case, an electrical connection was made by physically contacting probe tips to the LED die after laser transfer. In the ablative (DRL-L&P) case, timer chips, LED arrays, SMD resistors, and capacitors were successfully laser-transferred and functionally verified. Probe tips electrically powered these SMDs and IC chips to verify their functionality; alternatively, this technique also used LIFT to print metallic interconnects to an LED array on polyimide, which remained functional after laser transfer [19]. This is the only technique where the same tool could be used to both transfer the die and build the interconnections.

In the next section, the use of this technique to transfer and embed various discrete components, called "lase-and-place," is discussed. The performance of the components after the transfer are characterized and the transfer kinetics are examined. As mentioned earlier, this technique is a subset of LDW processes, which can be used to machine the pocket, transfer the component into the pocket, and make interconnections to the supporting circuit using essentially the same apparatus.

12.2.1 Lase-and-place

This technique was developed in 2007 as part of NRL's efforts to extend LDW processes to the fabrication of embedded electronic components and devices. The experimental setup is similar to other LIFT schemes using a donor and receiving substrate, as shown in Fig. 12.1.

The discrete components were attached, with the active side facing the laser pulse, to a sacrificial DRL layer coated on a laser-transparent donor substrate. The sacrificial layer could be a spin-coatable solution such as photoresist, wafer protective coating, or polyimide precursor. After attachment to the DRL, the donor substrate could be rinsed in a solvent to remove excess DRL material, resulting in components that are supported by "pedestals" on the donor substrate [18]. This geometry reduces the amount of adhesion between the component and the donor substrate and therefore decreases the transfer threshold fluence and minimizes the potential of damage. The donor substrate was then placed in close proximity to a receiving substrate. Upon exposure to a laser pulse, the sacrificial layer was ablated and the generated vapors were released, propelling the component away from its support toward the receiving substrate.

A wide range of devices and structures was successfully laser-transferred, as seen in Fig. 12.2. They included 0.3-mm^2 InGaN LED's, 1.2-mm^2 LM555 bare die, 2.6-mm^2 ASIC bare die, 0402 SMD (1 $\times$ 0.5 mm) components, and some MEMS-scale parts. The ability of the lase-and-place technique to place heterogeneous components onto the same substrate with the same tool (merely by using ribbons with different components) is an advantage this technique has over traditional pick-and-place tools, which must be adjusted to accommodate various shapes and sizes. In the lase-and-place technique, the shape and size of the laser spot can be adjusted to match each component by simply selecting the appropriate aperture. In addition, the versatility of the LDW technique was demonstrated by the laser-printed metal pattern in the center of Fig. 12.2(b). Details of the laser printing of metal interconnects are presented in Section 12.3.1.

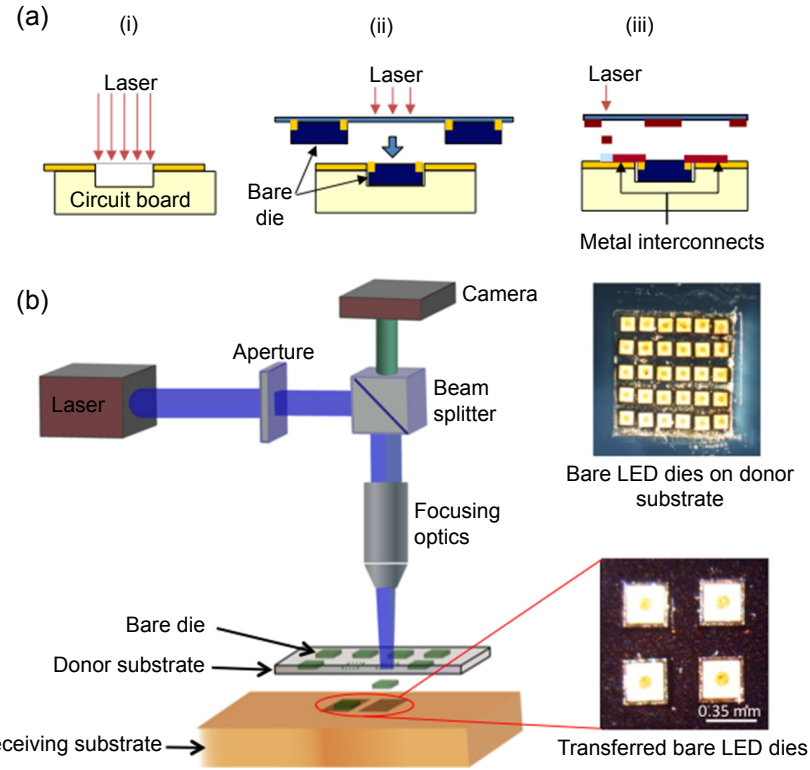

Figure 12.1 Schematic diagram (a) showing laser direct write (LDW) processes for embedding electronics: (i) micromachining, (ii) lase-and-place, and (iii) laser-induced forward transfer or laser transfer of functional materials. Some of the main components in the lase-and-place setup are shown in (b). *LED*, light-emitting diode.
Adapted and reprinted with permission from A. Piqué, N.A. Charipar, R.C.Y. Auyeung, H. Kim, S.A Mathews, Assembly and integration of thin bare die using laser direct-write, in: C.B. Arnold, et al. (Eds.), Proceedings of SPIE, San Jose, vol. 6458, 2007, pp. 645802-1−645802-10. © 2007 by SPIE.

The LM555 bare die (timer chip) and the LED were each tested for functionality after transfer. Many LM555 bare dies were tested with a probe station, and their output signals were identical to those before laser transfer. An embedded LED bare die was also electrically contacted with probe tips and displayed bright emission. A more robust demonstration of the laser transfer process is shown in Section 12.4 by a working array of embedded LED dies and interconnects, all made by L&P and laser printing.

Another advantage the L&P process has over pick-and-place machines is its ability to transfer ultrathin (10 μm) 1-mm^2 silicon substrates, as shown in Fig. 12.3. These substrates were transferred intact with a placement accuracy of better than 50 μm without any fracture. This accuracy could be improved by optimizing the DRL layer,

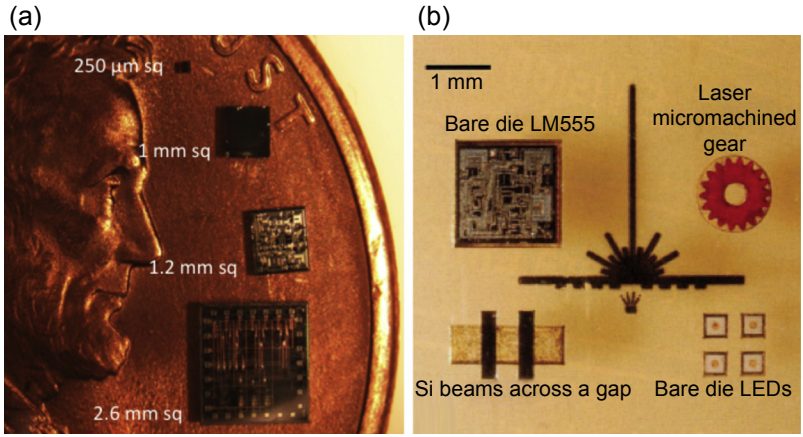

Figure 12.2 (a) Optical micrograph showing the various sizes of laser-transferred bare die and silicon substrates. The smallest device (top) is a bare die light-emitting diode measuring ~0.25 mm^2, whereas the larger device (bottom) measures 2.6 mm^2. (b) Optical image of various components transferred onto a plastic substrate by lase-and-place. The artwork in the center is a schematic illustration of the lase-and-place technique and was laser-printed using silver metallic nanoink.
Adapted and reprinted with permission from S.A. Mathews, N.A. Charipar, K. Metkus, A. Piqué, Manufacturing microelectronics using Lase-and-Place, Photonics Spectra 41(10) (2007) 70–74. © 2007 by Laurin Publishing.

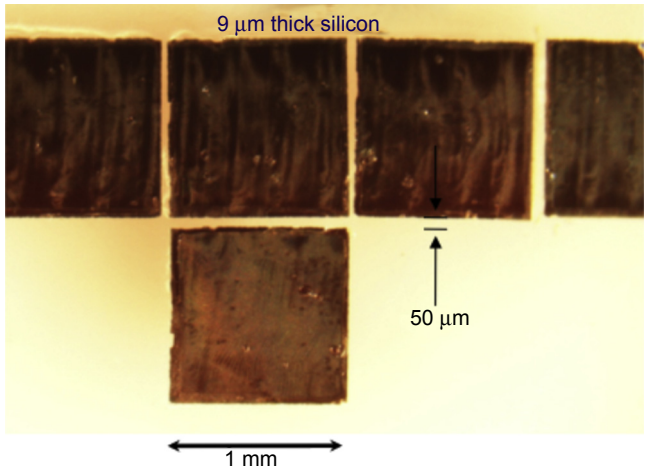

Figure 12.3 Optical micrograph showing laser transfer of adjacent 1-mm^2 ultrathin (10-μm-thick) silicon substrates demonstrating the placement accuracy and sensitive handling capability of the lase-and-place technique.
Adapted and reprinted with permission from A. Piqué, N.A. Charipar, R.C.Y. Auyeung, H. Kim, S.A Mathews, Assembly and integration of thin bare die using laser direct-write, in: C.B. Arnold, et al. (Eds.), Proceedings of SPIE, San Jose, vol. 6458, 2007, pp. 645802-1–645802-10. © 2007 by SPIE.

the donor−to−receiving substrate distance, and transfer laser parameters. The slight residue on the surface was probably polymer material from the DRL that remained after the transfer. These ultrathin substrates are beyond what is currently needed for RFID tags (50−100 μm thick), but the ability of the L&P process to transfer them without damage shows the viability of this technique in embedding and accurately placing ultrathin components.

A study of the kinetics of the laser transfer process were studied by stroboscopic imaging of the release and transfer of various discrete components from a donor substrate without a neighboring receiving substrate [17,18]. Video images of the laser release of a 1-mm^2 silicon tile, 1.4-mm^2 LM555 bare die, and a 2 × 1-mm SMD resistor are shown in Fig. 12.4. Note that the receiver substrate is typically ≪1 mm from the donor substrate, so any tilt or rotation of the transferred component would be negligible. An analysis of the component trajectories at transfer threshold showed that the velocities were approximately a few meters per second (for 1- and 2.6-mm^2 components).

An interesting application of the L&P technique was recently used to transfer thin solid metal interconnects (which could be considered as "discrete components" or "devices") to a series of millimeter-sized silicon capacitors. The laser transfer of embedded bare dies with the active side up makes the contact pads accessible for

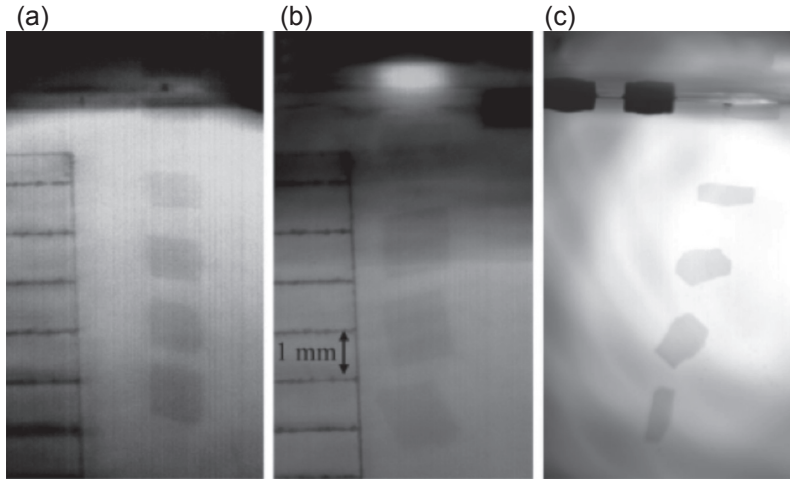

Figure 12.4 Multiple exposure optical micrograph of the laser release of (a) 1 × 1-mm silicon substrate, (b) 1.4 × 1.4-mm LM555 bare die, and (c) 2 × 1-mm surface-mount resistor device (SMT package 0402 series). The donor substrate can be observed at the top of each image. The time interval between exposures was adjusted for each image. For images (a) and (b) a glass ruler with 1-mm spacing between marks can be observed on the left.
Adapted and reprinted with permission from A. Piqué, N.A. Charipar, R.C.Y. Auyeung, H. Kim, S.A Mathews, Assembly and integration of thin bare die using laser direct-write, in: C.B. Arnold, et al. (Eds.), Proceedings of SPIE, San Jose, vol. 6458, 2007, pp. 645802-1−645802-10. © 2007 by SPIE.

interconnect assembly. These interconnects must be compact but yet able to accommodate a wide range of die sizes and shapes and display good electrical performance under varying conditions of thermal and mechanical stress (eg, temperature, vibration). A solid metal interconnect could be preferred over traditional wire bonds, which have a finite loop height above the substrate and could fail under high internal and external stress loads. Solid metal interconnects were recently bent by a laser and then laser transferred to span and connect a set of silicon capacitors, as shown in Fig. 12.5 [20]. Copper strips (1 mm × 100 μm × 12.5 μm thick) were first etched out of a copper foil attached to a donor substrate. This donor substrate was then placed over the capacitor pads and a laser pulse fired at the center of a strip resulting in a *U*-shaped bend in the copper, without releasing the strip. Next, a laser pulse was fired at the ends to transfer the entire copper strip to conductive epoxy pads (previously laser-printed) on the capacitors. The measured capacitance of the array of capacitors agreed with the expected value. This bend in the copper interconnect could accommodate mechanical or thermal stresses arising from component geometry mismatches or high electrical load. These early results indicate the potential of this technique to transfer even smaller and thinner interconnects that could be used in embedded electronics.

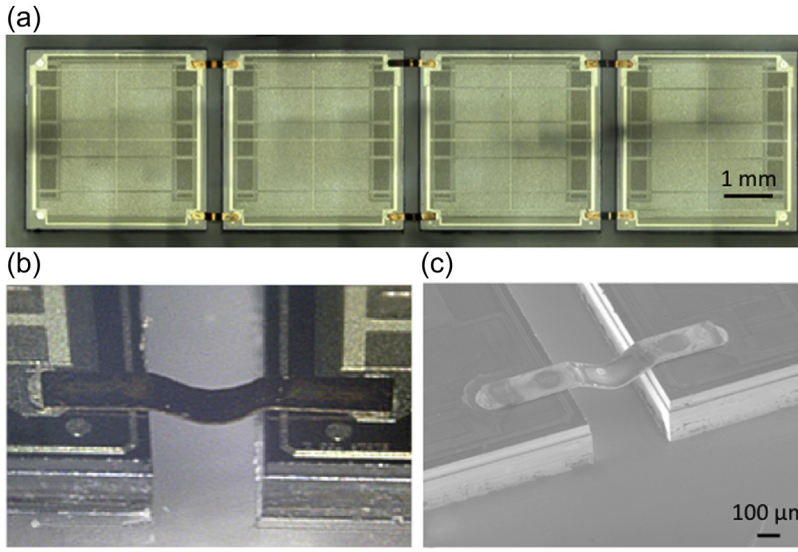

Figure 12.5 Optical micrographs of (a) an array of silicon capacitors interconnected with laser transferred, laser bent copper beams. Close-up view (b) of a single interconnect attached with conductive epoxy and (c) angled scanning electron microscopic view.
Adapted from Figs. 5 and 6 of S.A. Mathews, I. Beniam, N. Charipar, A. Piqué, Laser induced forward transfer (LIFT) for direct-write fabrication and assembly of microelectronics and reprinted with permission from 2015 ICALEO (34th International Congress on Applications of Lasers & Electro-optics) Conference Proceedings: Session LMF1, Paper M101 (October 2015), pp. 9−13. © 2015 by Laser Institute of America, Orlando, FL. All rights reserved.

L&P has been shown to be an additive manufacturing technique that surpasses the capabilities of typical pick-and-place tools by transferring and embedding miniature and ultrathin components without damage. The preserved functionality of devices during the transfer shows that the active-side-up orientation of the die is safe enough to withstand the low laser fluences used in the process. These low laser fluences can also be used to print functional materials and devices directly into a substrate to achieve an even higher level of miniaturization and embedding. The rest of this chapter discusses the use of LIFT to print complex solutions of functional materials for these embedded applications.

12.3 Laser-induced forward transfer of functional materials systems

As discussed in the introduction, LIFT can also be used to transfer functional materials directly into a substrate to form embedded devices. Traditionally, LIFT vaporizes a large portion of the donor film to transfer it to the substrate. Unfortunately, degraded functional properties, loss of feature resolution, and debris in the transfer are often the result. Instead, LIFT can be used with functional rheological fluid systems with a wide range of viscosities as the donor materials. The use of a fluid requires lower laser transfer fluence (<0.1 J/cm^2) and provides the advantages of improved functional properties, better feature resolution, and less debris. In the case of material with a very high viscosity, a novel form of LIFT called "laser decal transfer" (LDT) has even been used to fabricate freestanding interconnects and is discussed in detail next. Following that, additional examples of LIFT of functional materials (and devices), which could all be embedded in principle, are presented.

12.3.1 Laser-induced forward transfer of interconnects

LIFT was first used to transfer viscous fluids, pastes, or inks for the fabrication of metal interconnects, vias, and antenna structures [30,31]. By using a commercially available screen-printable silver ink, LIFT was used to print patterns in premachined trenches and even over a 3D surface (step). In this first demonstration, the laser spot size was adjusted to match the required line-width of the feature, and laser pulses were then used to "stitch" together a continuous line or pattern. The ink had a low enough viscosity that adjacent transferred features could merge together to ensure electrical continuity. Once completed, the transfers on the receiving substrate (usually a printed circuit board) were cured at $<150^{\circ}$C to increase its electrical resistivity. After curing, the transferred features displayed good adhesion and mechanical properties, as indicated by tape and flexing tests [30]. The ability to deposit conformal metal patterns on substrates at low temperatures also allowed for the fabrication of novel types of electronic designs such as conformal GPS antennas [32] on polymer radomes.

The next advance in LIFT came from the adoption of nanoparticle inks ("nanoink") that were undergoing extensive development for the inkjet printing industry.

By reducing the particle size (<100 nm), the printed resolution increased and the curing temperature decreased, which enabled fabrication on flexible substrates. However, these commercially available nanoinks typically have viscosities of ~15 cP (centipoise) to mitigate clogging issues with inkjet nozzles. If these nanoinks were used on the donor substrate without modification, then the transfers made by the LIFT process would suffer from the same issues as inkjet, namely, feature spreading caused by wetting interactions between the substrate and ink, satellite droplets ("splatter"), possible deleterious interactions between the solvent in the ink and the receiving substrate, and low mass of material deposited as a result of low solids content in the ink. By using heat or vacuum to increase the viscosity of the as-received inkjet silver ink before transfer, LIFT was used to print a pair of 25-μm-wide × 1-mm-long silver lines separated by only 50 μm, with high definition and without any debris [33,34]. The measured resistivity of these silver lines were ~12 times the bulk silver value after curing, and device performance was similar to those made by ebeam deposition. The resolution and length of these patterns demonstrated the capability of LIFT to print electrodes that met the critical dimension requirements in organic thin-film transistors.

Although increasing the viscosity of the as-received inkjet ink improved the quality of laser transfers, there was a limit to the amount of solvent removed from the ink and the maximum viscosity (~400 cP) achieved. A better way was to start with higher-viscosity nanoink for the donor layer. A silver nanoink with a viscosity ~10,000 cP was used to laser-print 19-μm-wide lines on polyimide [35]. A silver nanopaste, commercially produced for screen-printing, with viscosity ~100,000 cP, was used to laser-print 5-μm-wide lines on glass [36,37]. The as-transferred lines displayed excellent definition and resolution without any surrounding debris. After laser curing, these lines were measured to have a resistivity near two times that of bulk silver, demonstrating no significant loss of functional properties as specified by the manufacturer. The high viscosity of nanopaste allowed the transfer of patterns that were highly congruent in shape and size to the illuminated laser area on the donor layer. This high congruence led to naming this LIFT process LDT, and it allowed the laser transfer of patterns with feature fidelity and thickness uniformity comparable to lithographically patterned thin films. LDT is a unique form of LIFT in that ink−substrate interactions are minimal, functional properties are preserved in the transferred material (since minimal vaporization occurs), and the geometric dimensions of the transfer are identical to those of the incident laser spot with sharp edge definition.

The high fidelity of the transfer to the shape and size of the laser beam implies that the laser spot (and hence the transfer) can be arbitrarily shaped to the design element. Each transferred volume element (voxel) in the donor layer directly corresponds to a pixel in the two-dimensional design, thus enabling true digital microfabrication in the LIFT process. Not only does this minimize prototyping time, but the LDT process can process entire interconnects, transmission lines, pads, or perhaps an entire device such as a capacitor [38] with a single laser pulse. One of the early applications of LDT was for additive repair of defective metal patterns in liquid crystal displays [36]. Fabrication of arrays comprising individual split-ring elements was demonstrated for rapid prototyping of resonators for metamaterial applications [39]. The viscosity of silver

nanopaste was sufficiently high that silver microcantilevers and microbridges could be placed over a trench with a single laser pulse and remain freestanding without the use of any sacrificial layers [40,41]. Similarly, multilayer structures [38] and cavity-sealing membranes [42] have also been demonstrated via LDT. Such freestanding structures could not be generated by lithographic techniques without the use of sacrificial layers and demonstrates the unique capabilities of LDT among traditional direct-write processes.

The ability of LDT to create freestanding structures becomes extremely valuable in providing interconnects to embedded dies. These interconnects could bridge the narrow gap that typically surrounds the embedded component and/or accommodate any height differences between the die contact pads and the rest of the circuitry.

As demonstrated in Fig. 12.6, interconnects printed by LDT spanned across a gap and adapted to a ~15-μm height mismatch between an embedded LED die and a gold/polyimide substrate [43]. Light emission from the LED demonstrated the functionality of the interconnects even after 500 cycles of bending (13-mm radius). As shown in Fig. 12.7, the LDT process can be repeated over the same location to build 3D structures for crossover interconnect or via applications. In addition, by adjusting the laser transfer fluence, it is possible to fold the voxel along an edge, thus allowing interconnects alongside two orthogonal planes on the same substrate [44]. This ability has no parallel in lithography and can be used to generate top-to-side or top-to-bottom interconnects.

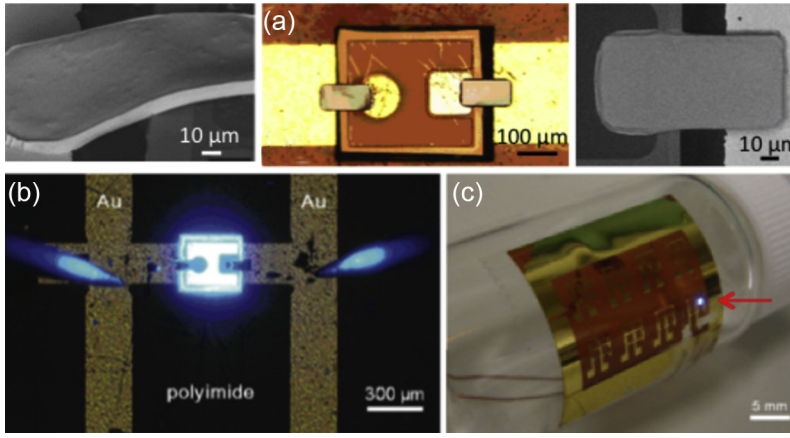

Figure 12.6 Optical micrograph showing (a) bare light-emitting diode (LED) die embedded inside a polyimide substrate connected with laser decal transferred silver interconnects. Left and right insets show scanning electron micrographs of interconnects spanning a gap; left interconnect "climbs" a height mismatch between the die and the substrate. (b) Optical micrograph showing LED emission powered through probe tips. (c) Optical micrograph of emission from the same LED device after 500 bending cycles.
Adapted and reprinted with permission from J. Wang, R.C.Y Auyeung, H. Kim, N.A. Charipar, A. Piqué, Three-dimensional printing of interconnects by laser direct-write of silver nanopastes, Advanced Materials 22 (40) (2010) 4462−4466. © 2010 by Wiley & Sons.

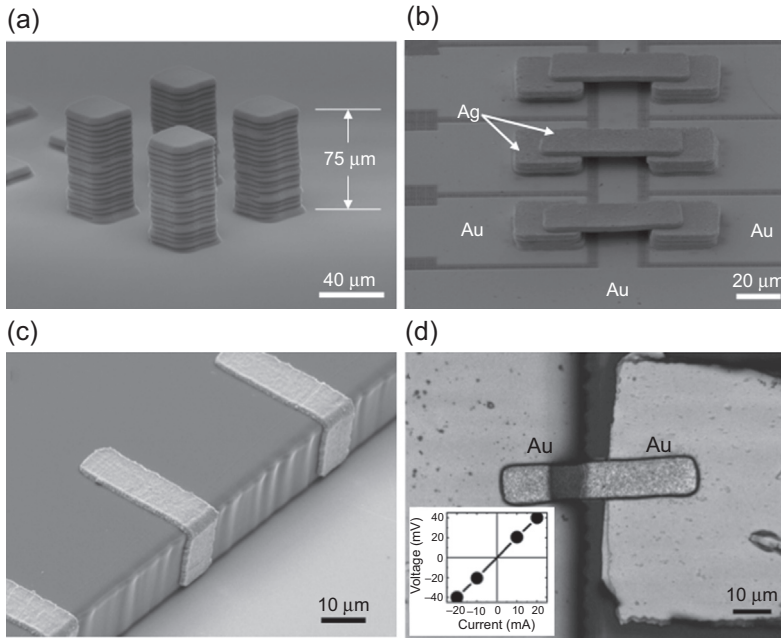

Figure 12.7 Scanning electron micrographs of silver interconnect structures made by laser decal transfer: (a) high aspect ratio micropillars on silicon, (b) crossover interconnect, (c) folded interconnect on a step edge printed with a single laser pulse by laser decal transfer. Confocal microscope image and (d) of a printed voxel connecting two gold (Au) electrodes separated by a 20-µm-high polymer (SU8) layer. Inset shows its I-V plot indicating ohmic behavior with a resistivity of ~7.3 µΩ-cm [4.6 times bulk silver (Ag)].
(a) and (b) Adapted and reprinted with permission from J. Wang, R.C.Y Auyeung, H. Kim, N.A. Charipar, A. Piqué, Three-dimensional printing of interconnects by laser direct-write of silver nanopastes, Advanced Materials 22 (40) (2010) 4462−4466. © 2010 by Wiley & Sons. (c) and (d) Adapted and reprinted with permission from H. Kim, M. Duocastella, K.M. Charipar, R.C.Y Auyeung, A. Piqué, Laser printing of conformal and multi-level 3D interconnects, Applied Physics A 113 (1) (2013) 5−8. © 2013 by Springer.

Solid metallic interconnects can also be laser transferred as was shown previously in Section 12.2.1. LIFT of conductive materials was combined with the L&P technique to transfer solid bent metal beams across a series of millimeter-sized capacitors. This hybrid technique shows promise in fabricating interconnects that can handle die-to-substrate height differences, high current loads, and thermal or mechanical strain arising from substrate movement.

12.3.2 Laser-induced forward transfer of materials for passives

LIFT could be used to directly fabricate and embed passive components into a substrate in a single step. Ideally, these printed components would retain all the functionality of discrete SMDs but with much smaller form factors.

Thick-film resistors satisfy a wide variety of electrical design requirements in hybrid microelectronics and are suitable for polymer substrates because of their low processing temperatures. LIFT was demonstrated for polymer thick-film resistors [45] and their resistance characterized for radiofrequency applications. The temperature coefficient of resistance of these printed resistors was measured to be similar to those made by screen-printing.

Dielectric materials present many challenges in their processing because of their brittleness, high processing temperatures, and microstructure-dependent properties. Nevertheless, LIFT was used to transfer a pad of 150-nm-diameter barium titanate particles in titania ink over an interdigitated capacitor structure on alumina and polyimide substrates [46]. After curing at 400°C, a dielectric constant of 50−55 with a loss tangent <2% were measured from 1 MHz to 1.5 GHz. It was shown that the dielectric properties of the ink were not affected by the transfer process.

LIFT of inductors was demonstrated by using an ink of $Y_3Fe_5O_{12}$ (YIG) powder dissolved in a poly(butyl methacrylate)/chloroform solution [47]. A four-turn flat YIG core (1.0×0.3 mm^2 $\times$ 20 μm thick) was laser-printed over patterned gold electrodes on a printed circuit board substrate. The measured inductance was 9 nH at 1 MHz and displayed high losses as a result of porosity in the YIG transfer.

An alternative laser-based method to fabricate an electronic circuit comprising several passive components and interconnects was demonstrated using low-temperature cofired ceramic technology [48]. LIFT was used to transfer silver, dielectric, inductor, and resistor paste onto green tape to form a multilayer laminated radiofrequency band pass filter. The measured center frequencies of the filters were near 1 GHz.

12.3.3 Laser-induced forward transfer of microbatteries

LIFT techniques have been used to print active electrochemical materials for the fabrication of electrochemical micropower sources, such as batteries and solar cells [49,50,51]. These micropower sources comprise three main components: a negative electrode (anode), a positive electrode (cathode), and an electrolyte/separator. Each of these components was typically assembled with a large degree of structural complexity, such as mixtures of electrochemically active materials, solid-state polymers, liquids, or nanocomposites. Thus the LIFT process must preserve the electrochemical activity and structural integrity of these components during the transfer.

One of the advantages of the LIFT process is that it allows for the deposition of highly porous, multicomponent materials without modifying their properties. These porous structures are an essential requirement for electrochemical devices, since enhanced contact between the electrodes and the electrolyte leads to better charge transfer, allowing a more complete utilization of the electrode materials. Another important feature of the LIFT process in fabricating electrochemical cells is the flexibility in the design of operating geometries. The simplest system is a planar structure where the electrodes of the cells are placed adjacent to each other in the same plane. Another geometry is to construct the cells in a stacked electrode. Both geometries have particular advantages and disadvantages. In the case of a stacked geometry, one can obtain higher areal densities, but each layer must be rigid enough to support the upper

layers while preserving their electrochemical properties. For a planar geometry, the fabrication process is much easier because it can handle softer and rougher materials, but they have higher internal resistances, resulting in low cell performance particularly at high currents. In addition, by combining LIFT of battery materials with laser-micromachined substrates, it is possible to further reduce the packaged size of an entire microdevice by embedding the cell components directly within a substrate while allowing its geometry to be adjusted to fit any form factor.

Planar alkaline microbatteries have been fabricated by laser printing zinc (as an anode), AgO_2 (as a cathode), and a KOH electrolyte in the form of complex suspensions or inks on various substrates [52,53]. Laser micromachining was subsequently used to provide clear electrical isolation between the electrodes. These planar microbatteries produced 0.6 mWh/cm^2 of energy density and 160 mWh/g of specific energy density [54]. Stacked microbatteries have also been demonstrated by LIFT. One challenge in fabricating the stacked batteries was printing the electrolyte. Since the use of a liquid electrolyte is limited by leakage and safety issues, it was important to replace the liquid electrolyte with a solid-state electrolyte. Our group at NRL developed a nanocomposite solid-polymer ionic liquid (nc-SPIL) as a solid-state electrolyte for the LIFT process [55,56,57]. The laser-printed nc-SPIL membranes exhibited the acceptable electrochemical behavior for ionic liquids, with a high conductivity of 1−3 mS/cm, while maintaining the strength and flexibility of the commonly used poly(vinylidenefluoride-hexafluoropropylene) (PVDF-HFP) copolymer binder. Thus, these laser-printed solid-state membranes were able to serve as both the electrolyte and separator [56]. LIFT has been used to print sequential layers of $LiCoO_2$ cathode, nc-SPIL electrolyte, and carbon anode into a laser micromachined pocket in a thin polyimide substrate to form an embedded all-solid-state lithium-ion microbattery. Although the total thickness of this stacked structure (30−50 μm) was much larger than sputter-deposited thin-film microbattery structures (1−5 μm), the stacked microbattery was thin enough to lie entirely inside the substrate. Fig. 12.8(a) and (b) shows a cross-sectional schematic diagram and a cross-sectional scanning electron micrograph of this embedded lithium (Li)-ion microbattery on a polyimide/aluminum substrate. As seen in Fig. 12.8(c) and (d), these embedded microbatteries charged/discharged more than 100 cycles at C/3 rate ($\sim$110 μA/cm^2) with an energy density of 1.32 mWh/cm^2 (or a specific energy of 330 mWh/g) [57].

Packaged Li-ion microbatteries were fabricated and then embedded into laser micromachined pockets in printed circuit boards. In this design, the $LiCoO_2$ cathode and the carbon anode were printed by LIFT on aluminum and copper current collectors, respectively, then assembled by placing the gel polymer electrolyte-soaked membrane between two electrodes. To package the batteries, the current collectors were sealed together with a thermally curable polymer spacer (Surlyn SF-71). The sealed batteries were then excised by the laser. Fig. 12.9(a) shows a cross-sectional scanning electron micrograph, showing individual layers of the packaged microbatteries made by LIFT. Fig. 12.9(b) shows a packaged Li-ion microbattery that was then embedded into the laser-machined pocket in the circuit board (Fig. 12.9(c)). The brown side in the microbattery is the copper-foil (anode) side (negative), while the silver side is the Al-foil (cathode) side (positive). Similarly packaged microbatteries made with thicker

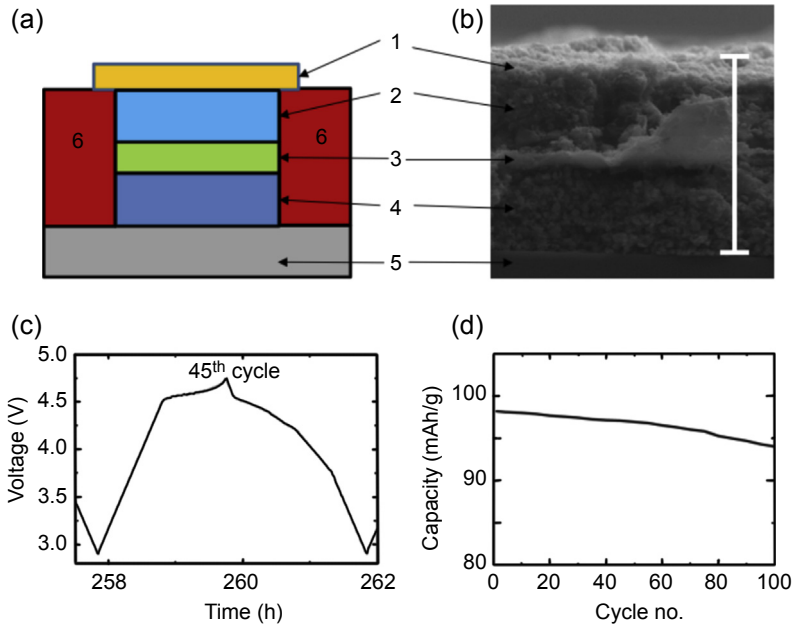

Figure 12.8 (a) Cross-sectional schematic diagram of an embedded lithium (Li)-ion microbattery (Pt/Carbon/nc-SPIL/$LiCoO_2$/Al). (b) Cross-sectional scanning electron micrograph of an embedded Li-ion microbattery. For both (a) and (b), 1 is the platinum metal deposited by sputtering, 2 is the carbon anode, 3 is the nanocomposite solid-polymer ionic liquid membrane, 4 is the $LiCoO_2$ cathode, 5 is the aluminum-current collector, 6 is the polyimide. The vertical scale bar is 30 μm. (c) and (d) Cycling performance of an embedded Li-ion microbattery. The battery was charged/discharged at C/3 rate (~110 μA/cm^2) between 4.2 and 3 V. The active electrode area was 3 × 3 mm.
(b) Adapted and reprinted with permission from T.E. Sutto, M. Ollinger, H. Kim, C.B. Arnold, A. Piqué, Laser transferable polymer-ionic liquid separator/electrolytes for solid-state rechargeable lithium-ion microbatteries, Electrochemical and Solid-State Letters 9 (2) (2006) A69−A71. © 2006 by The Electrochemical Society.

cathodes (~100 μm) showed excellent cycling performance over 100 cycles at low current density (0.1 mA/cm^2) with a discharge capacity of ~2.5 mAh/cm^2 [51], which was an order of magnitude higher than those achieved from sputter-deposited thin-film microbatteries with a 2.5-μm-thick $LiCoO_2$ cathode [58].

Using laser structuring to increase the active surface area of the laser-printed $LiCoO_2$ thick films for improved Li-ion diffusivity has been investigated [59,60]. Microbatteries fabricated with these laser-structured 3D cathodes exhibited improved capacity retention compared with those made with unstructured cathodes when cycling the batteries at C/5 rates (~100 μA/cm^2). After 100 cycles, the laser-structured electrodes showed a capacity of ~70 mAh/g, which was twice the remaining capacity of the unstructured cathode. This improvement was the result of the improved Li-ion diffusion paths and artificial porosity created by the laser structuring.

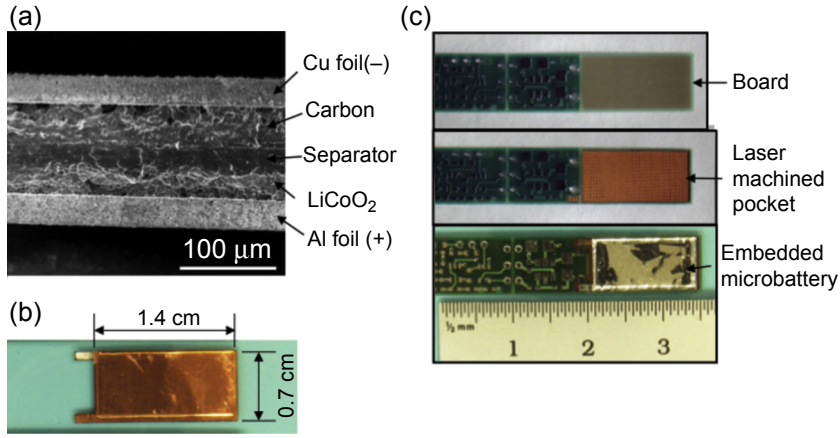

Figure 12.9 (a) Cross-sectional scanning electron micrograph of a packaged lithium (Li)-ion microbattery (Cu/Carbon/separator/$LiCoO_2$/Al). (b) Photograph of sealed Li-ion microbattery made by laser-induced forward transfer. (c) Photograph showing the starting circuit board that incudes an extra area for an embedded battery (top), laser machined pocket (middle), and the Li-ion microbattery embedded within the laser-machined pocket on the printed circuit board (bottom).

(a) Adapted and reprinted with permission from H. Kim, R.C.Y. Auyeung, A. Piqué, Laser-printed thick-film electrodes for solid-state rechargeable Li-ion microbatteries, Journal of Power Sources 165 (1) (2007) 413−419. © 2007 by Elsevier.

12.3.4 Laser-induced forward transfer of dye-sensitized solar cells

LIFT has been used to print porous nanocrystalline TiO_2 (nc-TiO_2) films to serve as active working electrodes for embedded energy-harvesting devices such as dye-sensitized solar cells [50]. These solar cells require a porous microstructure of an active TiO_2 layer with a large surface area so that a large number of dye molecules can be absorbed on the surface of the nanocomposite TiO_2 particles to achieve high efficiency. Under the right conditions, LIFT can print porous structures with large surface areas.

For LIFT of TiO_2 layers, the inks were prepared by mixing water-based colloidal suspensions of nanocomposite TiO_2 powders with organic additives. Mesoporous nanocomposite TiO_2 films were laser printed onto fluorine-doped tin oxide−coated glass substrates [50,61]. After sintering in the oven at 450°C, the TiO_2 electrodes were then soaked in the dye solution to coat the TiO_2 surface with dye molecules. The completed cells were assembled and sealed using a thermally curable polymer spacer (Surlyn) to separate the anode and cathode layers and to provide a reservoir for the I^{3-}/I^- electrolyte. Fig. 12.10(a) shows a schematic structure of a dye-sensitized solar cell. As seen in Fig. 12.10(b), the printed materials maintain a homogeneously distributed network of nanoparticles with a high degree of porosity. This 3D network of interconnected TiO_2 nanoparticles allows for good electron conduction,

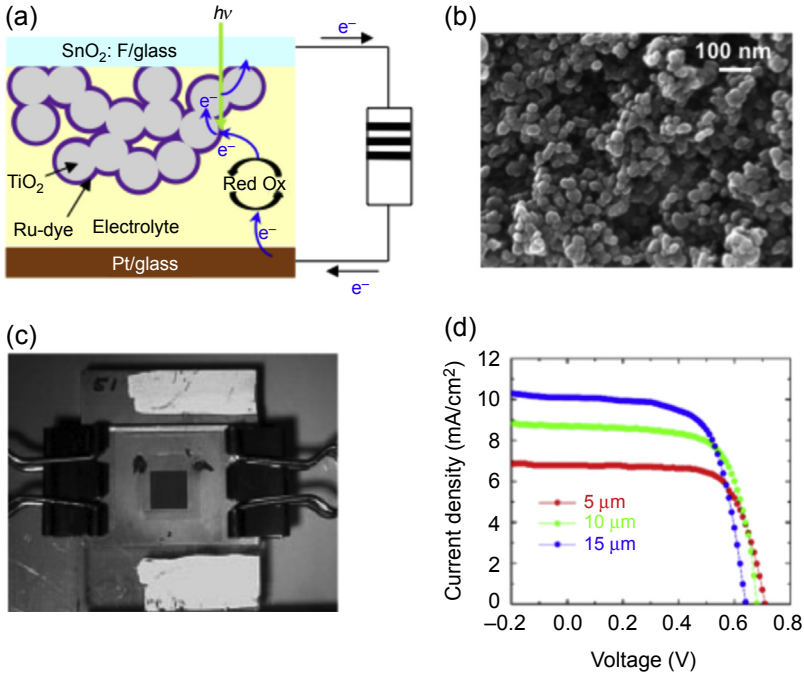

Figure 12.10 (a) Schematic cross-sectional diagram of a dye-sensitized solar cell. (b) Scanning electron micrograph of the surface of nanocomposite TiO_2 layer printed by laser-induced forward transfer on fluorine-doped tin oxide coated glass. The film was sintered at 450°C for 30 min. (c) Photograph of a packaged dye-sensitized solar cell fabricated with a laser-transferred nanocomposite TiO_2 electrode. (d) Current density versus voltage (J-V) of dye-sensitized solar cells fabricated by laser-based techniques with different thicknesses of active TiO_2 layers under a light intensity of 100 mW/cm^2 (AM 1.5 simulated solar illumination). The active cell area in all samples was 0.25 cm^2.

while the highly porous structure maximizes the amount of dye molecules adsorbed on the surface of the TiO_2 particles. Fig. 12.10(c) shows a photograph of a sealed dye-sensitized solar cell fabricated with the laser-printed nanocomposite TiO_2 electrode. Fig. 12.10(d) shows the current density (J) versus voltage (V) characteristics of dye-sensitized solar cells with three thicknesses of laser-printed nanocomposite TiO_2 layers. The short-circuit current density (J_{sc}) increases with the nanocomposite TiO_2 film thickness as a result of the increased surface area of the TiO_2 films, resulting in an increased amount of dye molecules. However, an increase of the TiO_2 thickness also increases defect/recombination sites, leading to an overall decrease in the open circuit voltage (V_{OC}). Thus the TiO_2 film thickness must be optimized to improve both J_{sc} and V_{OC} parameters jointly. The solar cells based on the optimized nanocomposite TiO_2 film ($\sim$15 µm) exhibit a light power conversion efficiency of $\sim$4.7%, which is comparable to those reported earlier for analogous cells fabricated with commercial TiO_2 powders (P25) using traditional screen-printing techniques [62,63].

The laser sintering process has also been explored to form a 3D network of TiO_2 nanoparticles for developing flexible dye-sensitized solar cells. To prepare the porous 3D network structures of TiO_2 working electrodes, printed TiO_2 electrodes must be sintered at relatively high temperatures ($\sim$450°C) to remove the organic additives to form an electrically connected nanostructure network within the mesoporous TiO_2 electrode. Laser sintering can form this connected network without causing any damage to flexible plastic substrates [61]. Typical laser sintering at IR wavelengths is not sufficient for TiO_2 because of its large band gap ($\sim$3.2 eV) and accordingly low absorption. However, the same UV source ($\lambda = 355$ nm) that was used for the LIFT of the nanocomposite TiO_2 inks can be used for the laser sintering of TiO_2 electrodes. The power conversion efficiency of the device based on the laser-sintered nanocomposite TiO_2 electrode is 1.8%, which is more than a twofold improvement from that of the device based on a non-laser-sintered TiO_2 electrode (0.7%). However, the 1.8% efficiency is still low compared with that of the standard cell (4.7%) fabricated with the high-temperature (450°C for 1 h) sintered nanocomposite TiO_2 electrode. This low efficiency indicates the insufficient necking of nanocomposite TiO_2 particles, which can be improved by further optimization of the laser sintering conditions. An advantage of this approach is that it allows both the transfer of the TiO_2 ink and in situ sintering of the mesoporous nanocomposite TiO_2 electrodes using the same UV laser, thus simplifying the steps required for fabricating dye-sensitized solar cells at low temperatures.

12.3.5 Laser-induced forward transfer of sensors

Chemical vapor sensors were the first type of sensor made by LIFT that relied on the ability of chemoselective polymers loaded with graphite particles to reversibly change its volume in the presence of vapors from a solvent [64,47]. Upon exposure, the chemoselective polymer (polyepichlorohydrin) expanded, which increased the average distance between its graphite particles and thereby increased its electrical resistance. Fig. 12.11(a) shows a photograph of a chemiresistor sensor element (black portion) laser printed across a set of silver interdigitated electrodes also fabricated by LIFT [65]. Fig. 12.11(b) displays the change in resistance as a function of time for this sensor element as it was challenged with vapors containing various concentrations of solvents (acetone in this case). Note that this sensor, which was entirely laser printed, was capable of detecting vapor traces down to the parts per million range and performed similar to one made by spray-coating.

Fig. 12.11(c) shows a fully operational chemiresistor sensor circuit with a chemiresistor sensor element, silver metal interconnects, and polymer thick-film resistors all made by LIFT [66]. The 4-Quad comparator device chip and the surface-mount LED components were soldered to the silver interconnects, and power to the circuit was provided by an external battery. In the presence of organic vapors, the resistance change across the chemiresistor sensor caused the 4-Quad comparator to sequentially light up individual LEDs, depending on the magnitude of the change in resistance across the sensor, proportional to the vapor concentration.

The NRL group has used LIFT to fabricate other small sensor devices such as temperature sensors [67], strain sensors on polyimide substrates [68], and simple

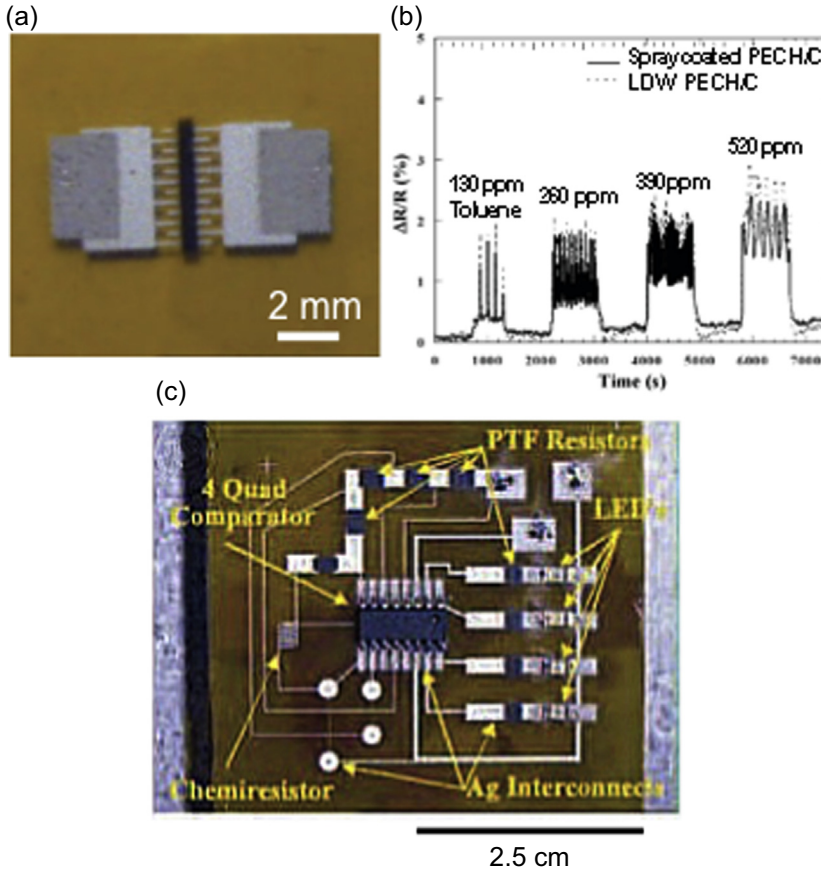

Figure 12.11 Example of an embedded chemical sensor fabricated using laser-induced forward transfer. (a) Chemiresistor gas sensor element (*black stripe*) and associated interdigitated silver metal electrodes (gray) on a polyimide substrate. (b) Change in resistivity with time for a laser-printed versus a spray-coated chemoselective sensor exposed to toluene. (c) Fully functional gas sensor circuit with a chemiresistor sensing element and light-emitting diode (LED) flashing indicators. *PECH*, polyepichlorohydrin; *PTF*, polymer thick film.
Adapted and reprinted with permission from A. Piqué, D.W. Weir, P.K. Wu, B. Pratap, C.B. Arnold, B.R. Ringeisen, R.A. McGill, R.C.Y. Auyeung, R.A. Kant, D.B. Chrisey, Direct-write of sensor devices by a laser forward transfer technique, in: Proceedings of SPIE, vol. 4637, 2002, pp. 361−368. © 2002 by SPIE.

electrochemical biosensors for the detection of small concentrations of dopamine on aqueous solutions [69]. Other groups have used laser-transfer techniques for depositing micropatterns of tin oxide layers with various oxygen ratios, which have potential application as gas sensors [70]. A capacitive chemical sensor array was recently produced using LIFT by laser transferring three different types of polymer materials sensitive to organic solvent vapors. Droplets of each polymer in solution were deposited

onto an array of thin silicon membranes to demonstrate a micromechanical capacitive vapor sensor [71,72].

12.3.6 Laser-induced forward transfer in parallel

Up to this point, the LIFT process has remained a serial direct-write process by nature, given the limited energy available from existing lasers. But the LIFT of fluids typically requires lower laser fluence (and energy) than traditional LIFT, so the laser beam could be expanded to print a larger area than just a small voxel. This would transform LIFT from a serial to a parallel printing technique and greatly increase its efficiency.

Nowhere is the parallel mode more useful than in the implementation of LDT (Section 12.3.1). Because the laser-transferred pattern in LDT is highly congruent to the dimensions of the incident laser spot, a spatial light modulator such as a commercial digital micromirror device (DMD) can impart an arbitrary shape to the laser beam, which would be exactly duplicated in the printed feature [73–75]. Thus the pixels in a DMD bitmap pattern would be "transformed" into the corresponding voxels of the laser-transferred pattern, creating a true "design-to-print" process. Combining the DMD's ability to quickly reload bitmap patterns with the synchronization of laser pulses and sample movement would result in a highly parallel, rapidly reconfigurable direct-write process.

Examples of the power of parallel direct-writing using DMD-LDT are shown in Fig. 12.12 [76]. In the laser printing of a grid (Fig. 12.12(a)), overlapping lines at the intersections would undergo bulging and loss of resolution if voxels were just stitched together serially, as in traditional LIFT, but with congruent LIFT and a DMD-shaped laser beam, the entire grid pattern can be printed with one single laser

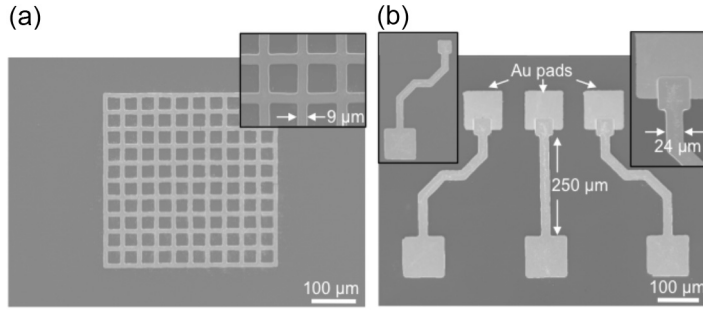

Figure 12.12 Scanning electron micrographs of the printing of a grid with (a) a single laser pulse and (b) three interconnects with three separate pulses using digital micromirror device—laser decal transfer. The left inset in (b) shows one type of interconnect; the right inset shows one end of the interconnect in contact with a pre-deposited gold (Au) pad on silicon. Adapted and reprinted with permission from A. Piqué, H. Kim, R.C.Y. Auyeung, A.T. Smith, Laser forward transfer of functional materials for digital fabrication of microelectronics, Journal of Imaging Science and Technology 57 (4) (2013) 040404. © 2013 by The Society for Imaging Science and Technology.

pulse [76]. In interconnect applications, DMD-LDT can print a pattern with a range of feature resolutions with a single pulse. Three types of interconnects in Fig. 12.12(b) were printed with three separate pulses, each pulse dynamically reconfigured for each interconnect type. These two examples demonstrate the ability of DMD to arbitrarily shape the laser pulse spatial profile and the ability of LDT to faithfully reproduce that profile in its transfer.

The combination of LDT with DMD is a potentially disruptive technology in the field of laser additive manufacturing since it transforms what was considered until now to be a serial process into a parallel printing technique. In fact, the well-established technology of DMD could "parallelize" other laser additive manufacturing techniques that require only low to moderate amounts of laser energy.

12.4 Laser-induced forward transfer of embedded circuit

At the board level, an embedded circuit could be broken down into discrete components (eg, SMDs, dies) and interconnects. In the preceding sections, successful laser-transfer and posttransfer functionality were demonstrated separately for discrete components (passives and actives), functional materials, and interconnects. Now, to demonstrate the full capability of all LDW processes together, all these components were transferred into one circuit board [77].

A simple blinker circuit comprising six passive SMD components (four resistors and two capacitors), two SMD LEDs, and one unpackaged integrated circuit (LM555 chipset in bare die form) was embedded in ULTEM, a thermoplastic polyetherimide substrate, using LDW, as shown in Fig. 12.13(a) and (b). Laser micromachining was used to excavate the pockets in the substrate that would contain each component. Once in place, the components were planarized with a layer of polyimide. The interconnects were made by laser micromachining blind vias through the polyimide to expose the contact pads on each device. The metal interconnects were then generated by laser printing a conductive silver ink. The resulting embedded circuit occupied a footprint smaller than a single packaged LM555 chip, as shown in Fig. 12.13(a). Fig. 12.13(b) shows a close-up of the LM555 chip with its laser-printed silver interconnects. It is estimated that these LDW embedded circuits can occupy footprints $\leq$1/4 and thicknesses $\leq$1/10 of those called out in a printed circuit board design, resulting in an overall circuit volume reduction of nearly two orders of magnitude. This shows that LDW processes can fabricate functional electronic circuits buried underneath the surface, with the surface or substrate serving as both circuit board and enclosure.

In Fig. 12.13(c), an array of blue LEDs was laser-transferred into laser-premachined pockets in a 125-μm-thick polyimide foil. After transfer, the LEDs were encapsulated by a polymer and then interconnected with laser-printed silver nanoink lines. In this demonstration, the entire circuit, consisting of the die and the interconnects (except for the power source), was laser transferred. The light emission from the LED array

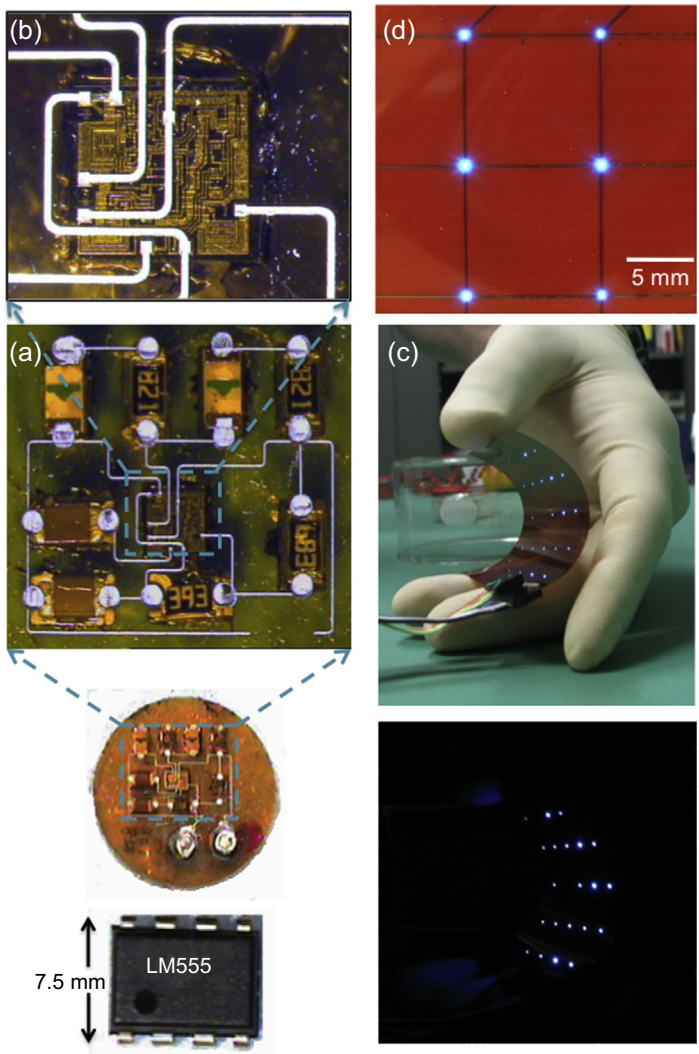

Figure 12.13 Embedded circuits made completely by laser direct write. (a) Optical micrograph of blinker circuit laser-embedded with resistor, light-emitting diode (LED), and capacitor surface-mount devices with an LM555 timing bare-die semiconductor chip in the center, shown to scale next to a packaged LM555 chip for size comparison. (b) Higher-magnification micrograph showing the laser-printed interconnects over the LM555 chip. (c) Array of embedded LEDs on a polyimide substrate. (d) Close-up view of emission of LEDs. (a) and (b) Adapted from A. Piqué, S.A. Mathews, B. Pratap, R.C.Y. Auyeung, B.J. Karns, S. Lakeou. Embedding electronic circuits by laser direct-write, Microelectronic Engineering 83 (11−12) (2006) 2527−2533. © 2006 by Elsevier. (c) and (d) Adapted and reprinted with permission from S.A. Mathews, N.A. Charipar, K. Metkus, A. Piqué, Manufacturing microelectronics using Lase-and-Place, Photonics Spectra 41(10) (2007) 70−74. © 2007 by Laurin Publishing.

embedded on a curved substrate in Fig. 12.13(c) demonstrated the viability of the laser transfer method in preserving the functionality of the LEDs and their interconnects on a flexed substrate.

12.5 Summary and outlook

Laser additive manufacturing is a promising technique for embedding electronics. Two approaches can be used: prefabricated discrete components (eg, SMDs, dies) can be laser transferred directly into a substrate or functional components (eg, interconnects, actives, passives) can be laser printed "on demand" into a substrate. LDW processes can provide all these additive processes as well as subtractive ones in a single tool. Subtractive processes such as laser micromachining are needed to remove material to create cavities for embedding and housing components inside a substrate. The advantage of using discrete components is that they are readily available components with the highest performance, and it is more reasonable to incorporate them into existing architecture rather than to "reinvent the wheel." Many laser-based techniques have been described for transferring these discrete components into a substrate, and some have more potential than others. The requirements for laser-transferring a small discrete component and especially a (thin) die are very stringent. The process or tool must impart just enough energy to release a die, propel it across a finite distance toward a receiving substrate, guide and place it without rotational/displacement error, and be useable for a wide range of die geometries. All of this must be done without degrading any of the die's functional properties, generating excess debris, or contaminating the die or surrounding substrate. Minimizing the laser transfer fluence ($\ll 1$ J/cm^2) is an important parameter that would enable many of these requirements to be satisfied.

LDW was used to successfully transfer and embed many discrete functional components into substrates at relatively low fluence. In addition, functioning interconnects, microbatteries, photovoltaics, and chemical sensors were directly printed from their constituent materials and offer an equivalent alternative to discrete components, depending on the application. These directly printed components would provide even smaller form factors than their discrete components and enable higher integration densities in embedded systems.

There is no doubt that much research is needed to develop new tools for reliably handling ultrasmall and ultrathin electronic components and integrating them into denser circuitry, especially at the packaging and systems level. Laser-based manufacturing is a unique tool that combines both additive and subtractive processes that could help fabricate and embed electronics into new geometries and structures for next-generation applications and technologies.

Acknowledgment

This work was funded by the Office of Naval Research through the Naval Research Laboratory Basic Research Program.

References

[1] J. Govaerts, W. Christiaens, E. Bosman, J. Vanfleteren, Fabrication processes for embedding thin chips in flat flexible substrates, IEEE Transactions on Advanced Packaging 32 (1) (2009) 77−83.
[2] R. Tummala, System scaling: the next frontier for a new era of electronic systems, Chip Scale Review 19 (5) (2015).
[3] R.D. Gerke, Embedded Passives Technology, NASA Report, NEPP, 2005.
[4] D.W. Lee, L. Li, S.X. Wang, J. Lu, C.P. Wong, S.K. Bhattacharya, J. Papapolymerou, Embedded passives, in: D. Lu, C.P. Wong (Eds.), Materials for Advanced Packaging, Springer, New York, 2009, pp. 459−502.
[5] R.M. Marks, Z. Hassan, K.Y. Cheong, Ultrathin wafer pre-assembly and assembly process technologies: a review, Critical Reviews in Solid State and Materials Sciences 40 (2015) 251−290.
[6] H.K. Charles, Advanced wire bonding technology: materials, methods, and testing, in: D. Lu, C.P. Wong (Eds.), Materials for Advanced Packaging, Springer, New York, 2009, pp. 113−179.
[7] J. Hoerber, J. Glasschroeder, M. Pfeffer, J. Schilp, M. Zaeh, J. Franke, Approaches for additive manufacturing of 3D electronic applications, Procedia CIRP 17 (2014) 806−811.
[8] M. Vaezi, H. Seitz, S. Yang, A review on 3D micro-additive manufacturing technologies, International Journal of Advanced Manufacturing Technology 67 (5−8) (2013) 1721−1754.
[9] C.B. Arnold, A. Piqué, Laser direct-write processing, MRS Bulletin 32 (1) (2007) 9−11.
[10] A. Piqué, D.B. Chrisey, Direct-Write Technologies for Rapid Prototyping Applications: Sensors, Electronics and Integrated Power Sources, Academic Press, San Diego, 2002.
[11] J. Bohandy, B. Kim, F.J. Adrian, Metal deposition from a supported metal film using an excimer laser, Journal of Applied Physics 60 (4) (1986) 1538−1539.
[12] F.E. Doany, C. Narayan, Laser release process to obtain freestanding multilayer metal-polyimide circuits, IBM Journal of Research and Development 41 (1−2) (1997) 151−157.
[13] R. Guerre, U. Drechsler, D. Jubin, M. Despont, Selective transfer technology for micro-device distribution, Journal of Microelectromechanical Systems 17 (1) (2008) 157−165.
[14] A.S. Holmes, S.M. Saidam, Sacrificial layer process with laser-driven release for batch assembly operations, Journal of Microelectromechanical Systems 7 (4) (1998) 416−422.
[15] N.S. Karlitskaya, D.F.D. Lange, R. Sanders, J. Meijer, Study of laser die release by Q-switched Nd:YAG laser pulses, in: Proceedings of SPIE, vol. 5448, 2004, pp. 935−943.
[16] N.S. Karlitskaya, J. Meijer, D.F.D. Lange, H. Kettelarij, Laser propulsion of microelectronic components: releasing mechanism investigation, in: Proceedings of SPIE, vol. 6261, 2006, 62612P.
[17] A. Piqué, N.A. Charipar, R.C.Y. Auyeung, H. Kim, S.A. Mathews, Assembly and integration of thin bare die using laser direct-write, in: C.B. Arnold, et al. (Eds.), Proceedings of SPIE, San Jose, vol. 6458, 2007, pp. 645802-1−645802-10.
[18] S.A. Mathews, R.C.Y. Auyeung, A. Piqué, Use of laser direct-write in microelectronics assembly, Journal of Laser Micro/Nanoengineering 2 (1) (2007) 103−107.
[19] S.A. Mathews, N.A. Charipar, K. Metkus, A. Piqué, Manufacturing microelectronics using 'Lase-and-Place, Photonics Spectra 41 (10) (2007) 70−74.
[20] S.A. Mathews, I. Beniam, N. Charipar, A. Piqué, Laser induced forward transfer (LIFT) for direct-write fabrication and assembly of microelectronics, in: 2015 ICALEO (34th

International Congress on Applications of Lasers & Electro-optics) Conference Proceedings: Session LMF1, Paper M101, 2015, pp. 9−13.
[21] V. Marinov, O. Swenson, R. Miller, F. Sarwar, Y. Atanasov, M. Semler, S. Datta, Laser-enabled advanced packaging of ultrathin bare diced in flexible substrates, IEEE Transactions on Components, Packaging and Manufacturing Technology 2 (4) (2012) 569−577.
[22] R. Miller, V. Marinov, O. Swenson, Z. Chen, M. Semler, Noncontact selective laser-assisted placement of thinned semiconductor dice, IEEE Transactions on Components, Packaging and Manufacturing Technology 2 (6) (2012) 971−978.
[23] V. Marinov, O. Swenson, Y. Atanasov, N. Schneck, Laser-assisted ultrathin die packaging: insights from a process study, Microelectronic Engineering 101 (2013) 23−30.
[24] V.R. Marinov, O. Swenson, Y. Atanasov, N. Schneck, Laser-assisted ultrathin die packaging: a route to a new class of microelectronic devices, in: Proceedings of SPIE, vol. 8608, 2013, 86080L-1 − 86080L-19.
[25] R. Saeidpourazar, R. Li, Y. Li, M.D. Sangid, C. Lu, Y. Huang, J.A. Rogers, P.M. Ferreira, Laser-driven micro transfer placement of prefabricated microstructures, Journal of Microelectromechanical Systems 21 (5) (2012) 1049−1058.
[26] R. Saeidpourazar, M.D. Sangid, J.A. Rogers, P.M. Ferreira, A prototype printer for laser driven micro-transfer printing, Journal of Manufacturing Processes 14 (2012) 416−424.
[27] E.E. Kuran, Y. Berg, M. Tichem, Z. Kotler, Integration of laser die transfer and magnetic self-assembly for ultra-thin chip placement, Journal of Micromechanics and Microengineering 25 (4) (2015), 045008.
[28] K. Li, M. Sparkes, W. O'Neill, Comparison between single shot micromachining of silicon with nanosecond pulse shaped IR fibre laser and DPSS UV laser, IEEE Journal of Selected Topics in Quantum Electronics 20 (5) (2014) 0900807 (Fig. 8).
[29] A. Al-okaily, P. Ferreira, Process performance of silicon thin-film transfer using laser micro-transfer printing, in: Proceedings of the ASME 2014 International Mechanical Engineering Congress and Exposition, vol. 2B, 2014 paper no. IMECE2014−37133, pp. V02BT02A043.
[30] A. Piqué, C.B. Arnold, B. Pratap, R.C.Y. Auyeung, H. Kim, D.W. Weir, Laser direct-write of metal patterns for interconnects and antennas, in: Proceedings of SPIE, vol. 4977, 2003, pp. 602−608.
[31] A. Piqué, B. Pratap, S.A. Mathews, B.J. Karns, R.C.Y. Auyeung, M. Kasser, M. Ollinger, H. Kim, S. Lakeou, C.B. Arnold, Laser direct-write of embedded electronic components and circuits, in: Proceedings of SPIE, vol. 5713, 2005, pp. 223−230.
[32] R.C.Y. Auyeung, M.W. Nurnberger, D.J. Wendland, A. Piqué, C.B. Arnold, A.R. Abbott, L.C. Schuette, Laser fabrication of GPS conformal antennas, in: Proceedings of SPIE, 5339, 2004, pp. 292−297.
[33] H. Kim, R.C.Y. Auyeung, S.H. Lee, A.L. Huston, A. Piqué, Laser forward transfer of silver electrodes for organic thin-film transistors, Applied Physics A: Materials Science and Processing 96 (2) (2009) 441−445.
[34] H. Kim, R.C.Y. Auyeung, S.H. Lee, A.L. Huston, A. Piqué, Laser-printed interdigitated Ag electrodes for organic thin film transistors, Journal of Physics D: Applied Physics 43 (8) (2010), 085101.
[35] R.C.Y. Auyeung, H. Kim, S.A. Mathews, A. Piqué, Laser direct-write of metallic nanoparticle inks, Journal of Laser Micro/Nanoengineering 2 (1) (2007) 21−25.
[36] A. Piqué, R.C.Y. Auyeung, K.M. Metkus, H. Kim, S.A. Mathews, T. Bailey, X. Chen, L.J. Young, Laser decal transfer of electronic materials with thin film characteristics, in: Proceedings of SPIE, vol. 6879, 2008, 687911.

[37] A. Piqué, R.C.Y. Auyeung, H. Kim, K.M. Metkus, S.A. Mathews, Digital microfabrication by laser decal transfer, Journal of Laser Micro/Nanoengineering 3 (3) (2008) 163−169.
[38] A.J. Birnbaum, H. Kim, N.A. Charipar, A. Piqué, Laser printing of multi-layered polymer/metal heterostructures for electronic and MEMS devices, Applied Physics A: Materials Science and Processing 99 (4) (2010) 711−716.
[39] H. Kim, J.S. Melinger, A. Khachatrian, N.A. Charipar, R.C.Y. Auyeung, A. Piqué, Fabrication of terahertz metamaterials by laser printing, Optics Letters 35 (23) (2010) 4039−4041.
[40] R.C.Y. Auyeung, H. Kim, A.J. Birnbaum, M. Zalalutdinov, S.A. Mathews, A. Piqué, Laser decal transfer of freestanding microcantilevers and microbridges, Applied Physics A: Materials Science and Processing 97 (3) (2009) 513−519.
[41] A.J. Birnbaum, R.C.Y. Auyeung, K.J. Wahl, M. Zalalutidnov, A.R. Laracuente, A. Piqué, Laser printed micron-scale free standing laminate composites: process and properties, Journal of Applied Physics 108 (8) (2010), 083526.
[42] A.J. Birnbaum, M. Zalalutdinov, K.J. Wahl, A. Piqué, Fabrication and response of laser-printed cavity-sealing membranes, Journal of Microelectromechanical Systems 20 (2) (2011) 436−440.
[43] J. Wang, R.C.Y. Auyeung, H. Kim, N.A. Charipar, A. Piqué, Three-dimensional printing of interconnects by laser direct-write of silver nanopastes, Advanced Materials 22 (40) (2010) 4462−4466.
[44] H. Kim, M. Duocastella, K.M. Charipar, R.C.Y. Auyeung, A. Piqué, Laser printing of conformal and multi-level 3D interconnects, Applied Physics A 113 (1) (2013) 5−8.
[45] R. Modi, H.D. Wu, R.C.Y. Auyeung, C.M. Gilmore, D.B. Chrisey, Direct writing of polymer thick film resistors using a novel laser transfer technique, Journal of Materials Research 16 (11) (2001) 3214−3222.
[46] D. Young, H.D. Wu, R.C.Y. Auyeung, R. Modi, J. Fitz-Gerald, A. Piqué, D.B. Chrisey, P. Atanassova, T. Kodas, Dielectric properties of oxide structures by a laser-based direct-writing method, Journal of Materials Research 16 (6) (2001) 1720−1725.
[47] A. Piqué, D.B. Chrisey, R.C.Y. Auyeung, J. Fitz-Gerald, H.D. Wu, R.A. McGill, S. Lakeou, P.K. Wu, V. Nguyen, M. Duignan, A novel laser transfer process for direct writing of electronic and sensor materials, Applied Physics A − Materials Science & Processing 69S (1999) S279−S284.
[48] C. Zhang, D. Liu, S. Mathews, J. Graves, T.M. Schaefer, B. Gilbert, R. Modi, H.D. Wu, D.B. Chrisey, Laser direct-write and its application in low temperature co-fired ceramic (LTCC) technology, Microelectronic Engineering 70 (1) (2003) 41−49.
[49] C.B. Arnold, R.C. Wartena, K.E. Swider-Lyons, A. Piqué, Direct-write planar micro-ultracapacitors by laser engineering, Journal of the Electrochemical Society 150 (5) (2003) A571−A575.
[50] H. Kim, G.P. Kushto, C.B. Arnold, Z.H. Kafafi, A. Piqué, Laser processing of nano-crystalline TiO_2 films for dye-sensitized solar cells, Applied Physics Letters 85 (3) (2004) 464−466.
[51] H. Kim, R.C.Y. Auyeung, A. Piqué, Laser-printed thick-film electrodes for solid-state rechargeable Li-ion microbatteries, Journal of Power Sources 165 (1) (2007) 413−419.
[52] A. Piqué, S.A. Mathews, R.C.Y. Auyeung, M. Ollinger, H. Kim, B. Pratap, C.B. Arnold, T.E. Sutto, Application of laser direct-write techniques for embedding electronic and micropower components, in: SPIE Proceedings, vol. 5662, 2004, pp. 564−569.
[53] A. Piqué, C.B. Arnold, H. Kim, M. Ollinger, T.E. Sutto, Rapid prototyping of micropower sources by laser direct-write, Applied Physics A: Materials Science and Processing 79 (4−6) (2004) 783−786.

[54] C.B. Arnold, H. Kim, A. Piqué, Laser direct write of planar alkaline microbatteries, Applied Physics A: Materials Science and Processing 79 (3) (2004) 417−420.
[55] M. Ollinger, H. Kim, T.E. Sutto, T.E. Martin, A. Piqué, Laser direct-write of polymer nanocomposites, Journal of Laser Micro/Nanoengineering 1 (2) (2006) 102−105.
[56] M. Ollinger, H. Kim, T.E. Sutto, A. Piqué, Laser printing of nanocomposite solid-state electrolyte membranes for Li micro-batteries, Applied Surface Science 252 (23) (2006) 8212−8216.
[57] T.E. Sutto, M. Ollinger, H. Kim, C.B. Arnold, A. Piqué, Laser transferable polymer-ionic liquid separator/electrolytes for solid-state rechargeable lithium-ion microbatteries, Electrochemical and Solid-State Letters 9 (2) (2006) A69−A71.
[58] J.B. Bates, N.J. Dudney, B. Neudecker, A. Ueda, C.D. Evans, Thin-film lithium and lithium-ion batteries, Solid State Ionics 135 (1−4) (2000) 33−45.
[59] H. Kim, J. Proell, R. Kohler, W. Pfleging, A. Piqué, Laser-printed and processed $LiCoO_2$ cathode thick films for Li-ion microbatteries, JLMN-Journal of Miro/Nanoengineering 7 (2012) 320−325.
[60] J. Pröll, H. Kim, A. Piqué, H.J. Seifert, W. Pfleging, Laser-printing and fs-laser structuring of $LiMn_2O_4$ composite cathodes for Li-ion microbatteries, Journal of Power Sources 255 (2014) 116−124.
[61] H. Kim, R.C.Y. Auyeung, M. Ollinger, G.P. Kushto, Z.H. Kafafi, A. Piqué, Laser-sintered mesoporous TiO_2 electrodes for dye-sensitized solar cells, Applied Physics A: Materials Science and Processing 83 (1) (2006) 73−76.
[62] S. Nakada, M. Matsuda, S. Kambe, Y. Saito, T. Kitamura, T. Sakata, Y. Wada, H. Mori, S. Yanagida, Dependence of TiO_2 nanoparticle preparation methods and annealing temperature on the efficiency of dye-sensitized solar cells, Journal of Physical Chemistry B 106 (2002) 10004−10010.
[63] M. Okuya, K. Nakade, S. Kaneko, Porous TiO_2 thin films systhesized by a spray pyrolysis deposition (SPD) technique and their application to dye-sensitized solar cells, Solar Energy Materials and Solar Cells 70 (2002) 425−435.
[64] A. Piqué, D.B. Chrisey, R.C.Y. Auyeung, S. Lakeou, R. Chung, R.A. McGill, P.K. Wu, M. Duignan, J. Fitz-Gerald, H.D. Wu, Laser direct writing of circuit elements and sensors, in: Proceedings of SPIE, 3618, 1999, pp. 330−339.
[65] A. Piqué, R.C.Y. Auyeung, J.L. Stepnowski, D.W. Weir, C.B. Arnold, R.A. McGill, D.B. Chrisey, Laser processing of polymer thin films for chemical sensor applications, Surface and Coatings Technology 163−164 (2003) 293−299.
[66] A. Piqué, D.W. Weir, P.K. Wu, B. Pratap, C.B. Arnold, B.R. Ringeisen, R.A. McGill, R.C.Y. Auyeung, R.A. Kant, D.B. Chrisey, Direct-write of sensor devices by a laser forward transfer technique, in: Proceedings of SPIE, vol. 4637, 2002, pp. 361−368.
[67] A. Piqué, C.B. Arnold, R.C. Wartena, D.W. Weir, B. Pratap, K.E. Swider-Lyons, R.A. Kant, D.B. Chrisey, Laser-induced forward transfer direct-write of miniature sensor and microbattery systems, in: SPIE Proceedings, vol. 4830, 2003, pp. 182−188.
[68] A. Piqué, C.B. Arnold, R.C. Wartena, B. Pratap, B. Shashishekar, K.E. Swider-Lyons, D.W. Weir, R.A. Kant, Laser direct-write of miniature sensor and microbattery systems, in: RIKEN Reviews, vol. 50, 2003, pp. 57−62.
[69] P.K. Wu, B.R. Ringeisen, D.B. Krizman, C.G. Frondoza, M. Brooks, D.M. Bubb, R.C.Y. Auyeung, A. Piqué, B. Spargo, R.A. McGill, D.B. Chrisey, Laser transfer of biomaterials: matrix-assisted pulsed laser evaporation (maple) and maple direct write, Review of Scientific Instruments 74 (4) (2003) 2546−2557.
[70] K. Komorita, T. Sano, H. Yamada, I. Miyamoto, Oxidation state control of micro metal oxide patterns produced by using laser-induced forward transfer technique, in: Proceedings of SPIE, vol. 4830, 2003, pp. 20−24.

[71] C. Boutopoulos, V. Tsouti, D. Goustouridis, S. Chatzandroulis, I. Zergioti, Liquid phase direct laser printing of polymers for chemical sensing applications, Applied Physics Letters 93 (19) (2008), 191109.
[72] V. Tsouti, C. Boutopoulos, D. Goustouridis, I. Zergioti, P. Normand, D. Tsoukalas, S. Chatzandroulis, A chemical sensor microarray realized by laser printing of polymers, Sensors and Actuators B: Chemical 150 (1) (2010) 148−153.
[73] R.C.Y. Auyeung, H. Kim, N.A. Charipar, A.J. Birnbaum, S.A. Mathews, A. Piqué, Laser forward transfer based on a spatial light modulator, Applied Physics A: Materials Science & Processing 102 (1) (2011) 21−26.
[74] R.C.Y. Auyeung, H. Kim, S.A. Mathews, A. Piqué, Laser forward transfer using structured light, Optics Express 23 (1) (2015) 422−430.
[75] R.C.Y. Auyeung, H. Kim, S.A. Mathews, A. Piqué, Spatially modulated laser pulses for printing electronics, Applied Optics 54 (31) (2015) F70−F77.
[76] A. Piqué, H. Kim, R.C.Y. Auyeung, A.T. Smith, Laser forward transfer of functional materials for digital fabrication of microelectronics, Journal of Imaging Science and Technology 57 (4) (2013), 040404.
[77] A. Piqué, S.A. Mathews, B. Pratap, R.C.Y. Auyeung, B.J. Karns, S. Lakeou, Embedding electronic circuits by laser direct-write, Microelectronic Engineering 83 (11−12) (2006) 2527−2533.